Hindawi Publishing Corporation
Journal of Nanomaterials
Volume 2011, Article ID 367156, 6 pages
doi:10.1155/2011/367156

Research Article

Room Temperature Ferromagnetism of (Mn,Fe) Codoped ZnO Nanowires Synthesized by Chemical Vapor Deposition

Yongqin Chang,[1] Pengwei Wang,[2] Qingling Sun,[1] Yongwei Wang,[1] and Yi Long[1]

[1] *School of Materials Science and Engineering, University of Science and Technology Beijing, Beijing 100083, China*
[2] *Department of Physics, National Key Laboratory of Mesoscopic Physics, Peking University, Beijing 100871, China*

Correspondence should be addressed to Yongqin Chang, chang@ustb.edu.cn

Received 28 March 2011; Accepted 28 August 2011

Academic Editor: Steve Acquah

(Mn,Fe) codoped ZnO nanowires were synthesized on silicon substrates in situ using a chemical vapor deposition method. The structure and property of the products were investigated by X-ray, electron microscopy, Raman, photoluminescence, and superconducting quantum interference device magnetometer. The doped nanowires are of pure wurtzite phase with single crystalline, and the elements distribute homogeneously in the doped nanowires. Photoluminescence spectrum of the doped nanowires is dominated by a deep-level emission with a negligible near-band-edge emission. The magnetic hysteresis curve with a coercive field of 35 Oe is clearly observed at 300 K, resulting from room-temperature ferromagnetic ordering in the (Mn,Fe) codoped ZnO nanowires, which has great potential applications for spintronics devices.

1. Introduction

Diluted magnetic semiconductors (DMSs) have stimulated great interest in recent years due to their potential applications in spintronics devices, where the spin degree of freedom of the electron is utilized in addition to its carrier concentration [1–3]. A promising technique is to use DMS to inject spin-polarized carriers into nonmagnetic semiconductor, and it is very important that the DMS materials have room temperature ferromagnetic property for the practical applications. ZnO doped with transition metals is one of the most promising DMS candidates, as it was predicted to be ferromagnetic above room temperature [1, 4], and some room temperature ferromagnetic materials have been successfully synthesized by several groups [5–7]. To integrate the ZnO-based DMSs into present electronics, it is reasoned that the combination of low dimensionality and room-temperature ferromagnetism in diluted magnetic oxides would generate new functional nanomaterials useful for future spintronics nanodevices. Some efforts have been focused on this kind of material, such as the fabrication of Mn-doped ZnO nanorods arrays [8] and Co-doped ZnO nanoneedle arrays [9]. Recently, several codoped DMS materials have been reported with the expectation that codoping can lead to remarkable improvement in the properties of DMS [10, 11]. Chakrabarti et al. reported that the saturation magnetic field can be enhanced by doping addition 2% Fe in the Mn-doped ZnO system [12]. Codoped Mn and Fe in ZnO nanostructures may contribute the local magnetic moments and enhancement of the charge carrier density. To the best of our knowledge, there was no research presented on Mn- and Fe-codoped ZnO nanostructures. In this letter, magnetization above room temperature has been achieved in (Mn,Fe) codoped ZnO nanowires prepared by a chemical vapor deposition (CVD) route.

2. Experiments

The fabrication process of the chemical vapor deposition is similar to our previous reports [13]. A gold film with thickness of 2 nm acting as catalyst was sputtered on a cleaned silicon substrate. In a typical synthesis, Zn, Mn, and Fe powders were put in a small alumina boat to serve as source materials. Silicon wafer was placed above the source at a vertical distance of 5 mm with its gold side facing downwardly. Then, the alumina boat was transferred into

the center of a horizontal alumina furnace. Argon with a flow rate of 30 sccm (standard-state cubic centimeter per minute) was supplied as the carrier gas in the furnace during heating. When the temperature at the center of the furnace reached 810°C, 5 sccm of oxygen was introduced. The furnace was held at 810°C for 2 h to synthesize the nanowires. During the whole growth process, the pressure of the system was maintained at atmospheric pressure without using pumping system. After the furnace was cooled down to room temperature, a yellowish film was observed on the silicon substrate. ZnO nanowires were synthesized at the similar condition only with Zn powder as the evaporation source.

X-ray diffraction (XRD) experiments were carried out with a X'pert MRD-Philips diffractometer using CuKa radiation. The micromorphology, structure, and composition of the products were studied using transmission electron microscopy (TEM, JEM-2010) and energy dispersive X-ray spectroscopy (EDXS). Elemental mapping was investigated by JEM-2100F microscope. Photoluminescence (PL) spectroscopy was performed at room-temperature, using a He-Cd laser of 325 nm wavelength as the excitation source. Room-temperature unpolarized Raman spectra were excited with a 514.5 nm Ar^+ laser, taken under backscattering geometry. Magnetization measurements were checked by means of a superconducting quantum interference device (SQUID, MPMS XL-7) magnetometer.

3. Results and Discussion

Figure 1 displays the indexed XRD pattern of the products, and the position and relative intensity of the diffraction peaks of both (Mn,Fe) codoped ZnO and pure ZnO nanowires are indexed to wurtzite ZnO structure. The XRD results of the (Mn,Fe) codoped ZnO nanowires demonstrate that the structure of the ZnO matrix is not changed by doping of Mn and Fe. The lattice constants measured from the XRD of the products are $a = 0.3252$ nm and $c = 0.5211$ nm, which are a little larger than those of pure ZnO ($a = 0.3250$ nm and $c = 0.5206$ nm). The ionic radius of Zn^{2+}, Mn^{2+}, Mn^{3+}, Fe^{2+}, and Fe^{3+} are 0.74, 0.80 0.66, 0.74, and 0.64 nm, respectively. Zn ions replaced with Fe and Mn may result in the changing in lattice constants, and it also indicates that there is few Mn^{3+} and Fe^{3+} in the (Mn,Fe) coped ZnO nanowires, because the lattice constants increase slightly compared with those of pure ZnO.

Figure 2(a) shows the typical TEM image of the (Mn,Fe) codoped ZnO nanowires, and it reveals that the mean diameter of the nanowires is around 65 nm with lengths up to several micrometers. High-resolution TEM (HRTEM) images show that the doped nanowires are of single-crystalline nature, and the lattice fringe spacing of 0.247 nm corresponds to the d value of (101) planes (Figure 2(b)). No any particle-like features were observed in the examined nanowires. The EDXS analysis reveals the existence of Mn and Fe ions in the ZnO samples, and the content of Mn and Fe are 6 at.% and 2 at.%, respectively. Elemental mapping was carried out to investigate the element distribution in the doped nanowires. The typical EDX elemental mapping

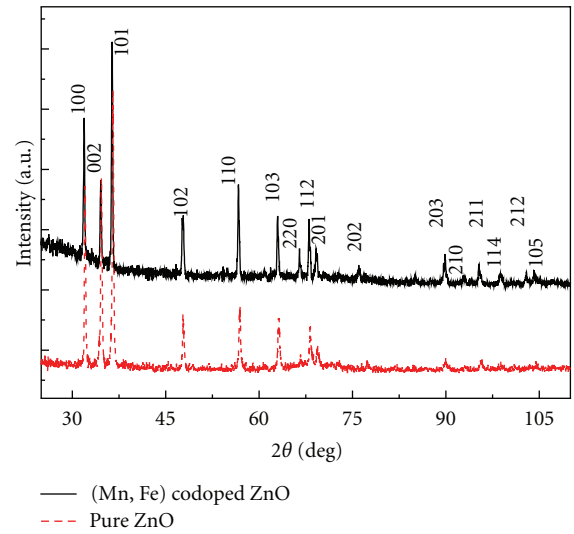

Figure 1: XRD pattern of the (Mn,Fe) codoped ZnO (solid line) and pure ZnO nanowires (dash line).

images of an individual (Mn,Fe) codoped ZnO nanowire were illustrated in Figure 3. These results show the shape of nanowire without any partial aggregation, which means that Mn and Fe distribute homogeneously in the nanowire instead of forming any oxide fine particles. Figure 3(d) shows that the profile of O is broader than those of the other elements, the reason is that O element was also absorbed by the supporting carbon film on the TEM grid and displaced in the profile.

The wurtzite ZnO structure belongs to the spaced group C_{6V}^4, and the optical phonon irreducible representation is $2A_1 + 2B_1 + 2E_1 + 2E_2$. Both the A_1 and E_1 modes are polar and split into transverse optical (TO) and longitudinal optical (LO) phonons. Nonpolar E_2 modes are Raman active, while B_1 modes are Raman inactive. Their phonon frequencies of the Raman spectra in ZnO are $A_{1(\mathrm{TO})} = 380\,\mathrm{cm}^{-1}$, $A_{1(\mathrm{LO})} = 574\,\mathrm{cm}^{-1}$, $E_{1(\mathrm{TO})} = 407\,\mathrm{cm}^{-1}$, $E_{1(\mathrm{LO})} = 583\,\mathrm{cm}^{-1}$, $E_{2(\mathrm{High})} = 437\,\mathrm{cm}^{-1}$, and $E_{2(\mathrm{Low})} = 101\,\mathrm{cm}^{-1}$ [14], respectively. The frequency of $330\,\mathrm{cm}^{-1}$ is the second-order spectrum arising from zone-boundary phonons 2-E_2(M) of ZnO [15]. The room temperature Raman spectra ranging from 200 to $850\,\mathrm{cm}^{-1}$ was presented in Figure 4. For the pure ZnO nanowires, the mode at $436.9\,\mathrm{cm}^{-1}$ with the strongest intensity is ascribed as $E_{2(\mathrm{high})}$ phonon mode, which is the typical Raman peak of ZnO bulk. $E_{2(\mathrm{high})}$ mode was usually used to understand the stress-induced phenomena in wurzite ZnO structures. As it is well known, an increase in the $E_{2(\mathrm{high})}$ phonon frequency is ascribed to compressive stress, whereas a decrease in the $E_{2(\mathrm{high})}$ phonon frequency is ascribed to tensile stress [16]. Compared with the frequency branch of $E_{2(\mathrm{high})}$ phonon of ZnO ($436.9\,\mathrm{cm}^{-1}$), the line center position of $E_{2(\mathrm{high})}$ phonon for the (Mn,Fe) codoped ZnO nanowires is observed at $434.9\,\mathrm{cm}^{-1}$, a Raman shift of $2.0\,\mathrm{cm}^{-1}$ had taken place, which indicates that a tensile stress was introduced in the nanowires because of the difference ionic radius between Mn, Fe, and

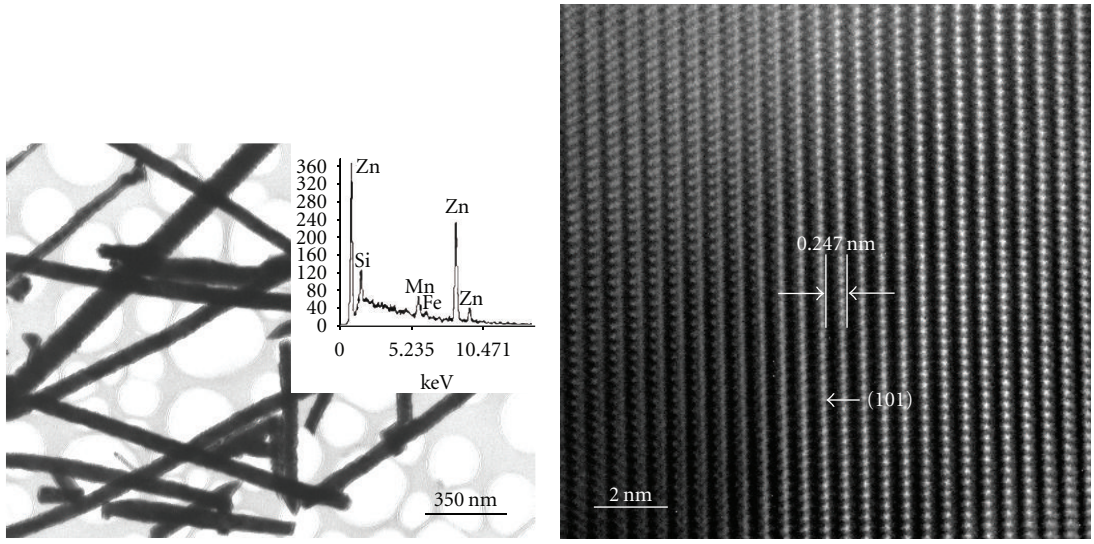

(a) (b)

Figure 2: (a) Typical TEM image of the (Mn,Fe) codoped nanowires, and the inset is the EDS pattern. (b) HRTEM image of the (Mn,Fe) codoped ZnO nanowires, revealing the single crystalline.

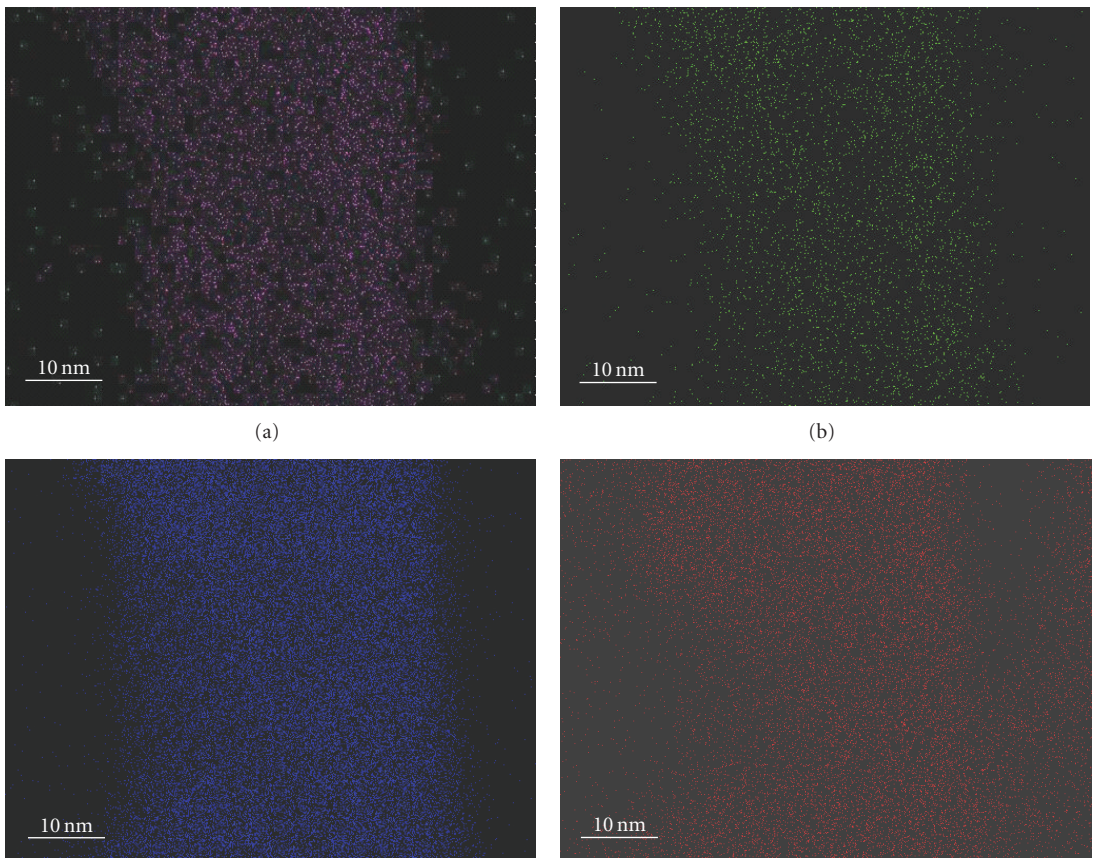

(a) (b)

(c) (d)

Figure 3: Elemental mapping images for the nanowire with Mn (a), Fe (b), Zn (c), and O (d).

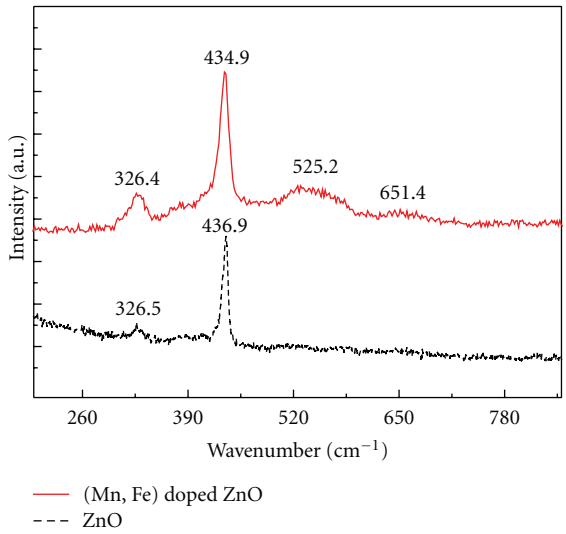

Figure 4: Raman spectra of the (Mn,Fe) codoped ZnO nanowires and pure ZnO nanowires.

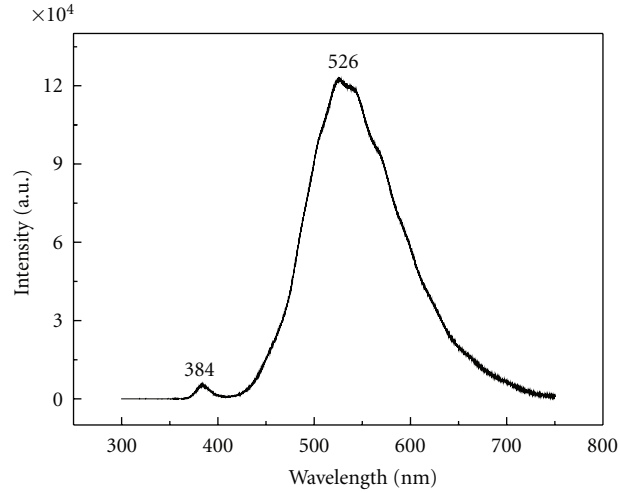

Figure 5: PL spectrum of the (Mn,Fe) codoped ZnO nanowires excited at room temperature.

Zn. The strongest intensity of $E_{2(\text{high})}$ phonon frequency for the (Mn,Fe) codoped ZnO nanowires also means that the wurtzite structure is preserved in spite of the inclusion of the Mn and Fe ions, which is consistent with the XRD results. The phonon mode centered at 326.5 cm^{-1} for ZnO and 326.4 cm^{-1} for (Mn,Fe) codoped ZnO are second-order spectra feature, which originates from the zone-boundary phonons of 2-E_2(M) for ZnO [15]. In the Raman spectrum of the (Mn,Fe) codoped ZnO nanowires, there are two additional broad Raman bands at around 525.2 cm^{-1} and 651.4 cm^{-1}, respectively. The vibration mode at 651.4 cm^{-1} was not presented in the ZnO films and single crystals, while it has been observed in Mn doped ZnO materials, where it was ascribed as local vibrational modes due to the intrinsic host-lattice defects [17]. In our experiments, when Mn and Fe atoms occupy the Zn sites, some new lattice defects are introduced or intrinsic host-lattice defects become activated due to the difference radius of Mn, Fe, and Zn. So, we guess that the vibration mode at 651.4 cm^{-1} associated with the defects was induced by Mn and Fe substitution. The mode at 525.2 cm^{-1} was also detected in other Mn single and Mn codoped with other magnetic ions ZnO films and nanostructures prepared by other groups [18, 19], and this mode has been reported correlated with Mn-related local vibration. The above Raman analysis shows that only ZnO phase is obtained, and a tensile stress is introduced because of the doping of Mn and Fe.

Room temperature photoluminescence spectra of the as-synthesized products were measured with excitation wavelength of 325 nm. As shown in Figure 5, the PL spectrum of the (Mn,Fe) codoped ZnO nanowires is similar to many reported data of ZnO. The luminescence band centered at 384 nm assigns to the ultraviolet (UV) excitonic emission, corresponding to the band emission of ZnO. The green luminescence band was generally attributed to the single ionized oxygen vacancies [20]. Up to now, we have not seen any reports on the photoluminescence of FeO, Fe_2O_3, Fe_3O_4, Mn_2O_3, and Mn_3O_4. A published report showed that MnO crystal shows the excitation spectra of the emission bands centered at 1.25 eV (992 nm) and 1.66 eV (747 nm) [21]. Figure 5 obviously shows that the green emission (526 nm) of the (Mn,Fe) codoped ZnO nanowires is not originated from MnO. From above results, we can conclude that the strong green emission (526 nm) was merely due to defects in the doped ZnO nanowires instead of from secondary inclusions. The broad band with the strong intensity of the green emission indicates that there exist many oxygen vacancies in the doped materials. The doping of Mn and Fe may affect the emission of ZnO. The high emission intensity of the near band emission only is observed in high crystal quality of ZnO [22]. If the material is of degraded quality, the exciton lifetime would be very short due to the additional scattering by defects, and the PL spectrum would be dominated by deep level emission. Mn and Fe dopants may introduce some defects and stress, which have been confined by the Raman spectra (Figure 4). The strong green emission in Figure 5 may result from the high quantity of oxygen vacancies and the defects originated from the dopants and the growth process.

The magnetic behavior of the doped materials is of critical importance for spintronics applications. Applied field-dependent magnetization (M-H) measurements of the (Mn,Fe) codoped ZnO nanowires were performed at 5 and 300 K, respectively. The diamagnetic response of the silicon substrate was subtracted from the magnetization plots. In Figure 6(a), the appearance of a well-defined loop with a coercive field of about 115 Oe signifies the (Mn,Fe) codoped ZnO nanowires being ferromagnetic at 5 K. Figure 6(b) shows the magnetic hysteresis curve measured at 300 K. The saturated magnetization M_s and coercive field H_c are 0.4 emug^{-1} and 35 Oe, respectively. Although the magnetization at 300 K is relatively weak compared with the value measured at 5 K, the hysteresis loop was clearly observed at 300 K, resulting from room-temperature ferromagnetic ordering in the (Mn,Fe) codoped ZnO nanowires. Recent

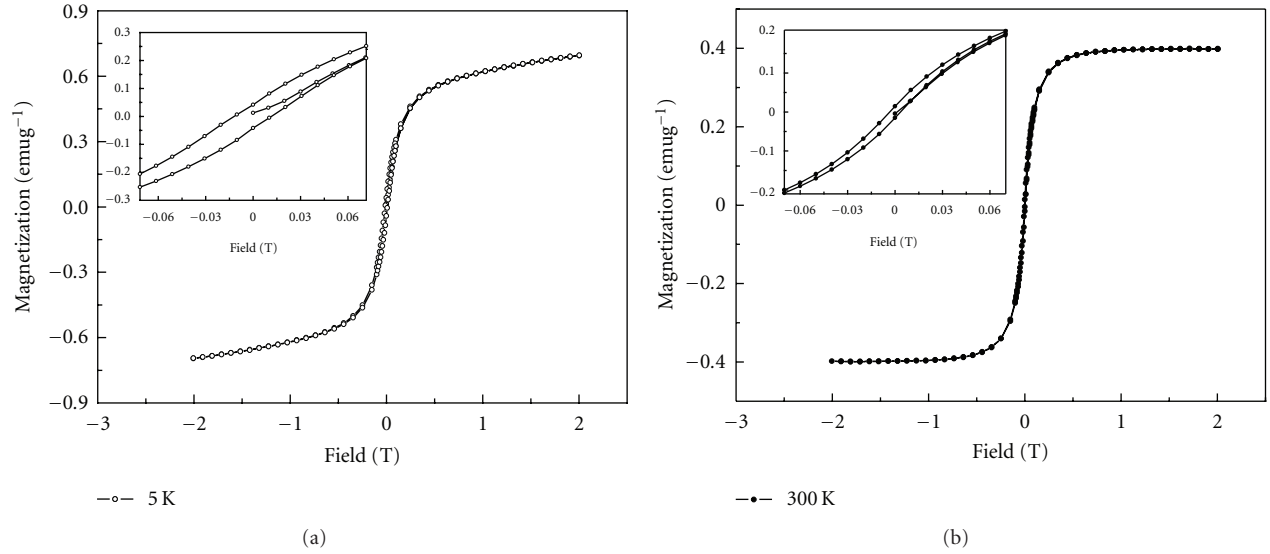

Figure 6: Hysteresis loops for the (Mn,Fe) codoped ZnO nanowires measured at 5 (a) and 300 K (b), and the corresponding insets show the enlarged parts of the *M*-*H* curves.

works reported that the ferromagnetism in the ZnO-based DMS controlled by the concentration of oxygen vacancies [23], and the enhancement of ferromagnetism was strongly correlated with the increase of oxygen vacancies in ZnO [24]. The PL measurements in our case demonstrate that there exist many oxygen vacancies in the doped materials. The room-temperature ferromagnetism of the (Mn,Fe) doped ZnO nanowires might originate from the super exchange interaction between nearest neighbor distance of magnetic ions (via oxygen vacancies). The role of Mn and Fe will be further investigated in the future.

4. Conclusions

This paper reported on the synthesis, characterization, and magnetic property of the (Mn,Fe) codoped ZnO nanowires through a chemical vapor deposition method. The XRD and Raman results show that the products are composed of pure wurtzite ZnO phase. HRTEM image indicates that the nanowires are of singe crystalline, and the elemental mapping profiles of the single nanowires show that the elements distribute homogeneously along the doped nanowires. Ferromagnetic behavior was obtained in the (Mn,Fe) codoped ZnO nanowires at low temperature as well as at room temperature. Our experimental results reveal that Mn and Fe incorporated into ZnO develop a room-temperature diluted magnetic semiconductor, which represents an important method for fabrication of transition metal-doped ZnO nanostructures with room-temperature ferromagnetic behavior.

Acknowledgments

This project is financially supported by Beijing Natural Science Foundation (no. 1092014), Open Project of Key Laboratory for Magnetism and Magnetic Materials of the Ministry of Education, Lanzhou University (LZUMMM2010002), and Metallurgy Foundation of University of Science and Technology Beijing. Y. Q. Chang is supported by Program for New Century Excellent Talents in University (no. NCET-07-0065) and Beijing Novel Program.

References

[1] A. H. Macdonald, P. Schiffer, and N. Samarth, "Ferromagnetic semiconductors: moving beyond (Ga,Mn)As," *Nature Materials*, vol. 4, no. 3, pp. 195–202, 2005.

[2] J. B. Yi, H. Pan, J. Y. Lin et al., "Ferromagnetism in ZnO nanowires derived from electro-deposition on AAO template and subsequent oxidation," *Advanced Materials*, vol. 20, no. 6, pp. 1170–1174, 2008.

[3] N. H. Hong, J. Sakai, N. Poirot, and V. Brizé, "Room-temperature ferromagnetism observed in undoped semiconducting and insulating oxide thin films," *Physical Review B*, vol. 73, no. 13, Article ID 132404, 4 pages, 2006.

[4] T. Dietl, H. Ohno, F. Matsukura, J. Cibert, and D. Ferrand, "Electric-field control of ferromagnetism," *Science*, vol. 287, no. 6815, pp. 1019–1022, 2000.

[5] P. Sharma, A. Gupta, K. V. Rao et al., "Ferromagnetism above room temperature in bulk and transparent thin films of Mn-doped ZnO," *Nature Materials*, vol. 2, no. 10, pp. 673–677, 2003.

[6] T. S. Herng, D. C. Qi, T. Berlijn et al., "Room-temperature ferromagnetism of Cu-doped ZnO films probed by soft X-ray magnetic circular dichroism," *Physical Review Letters*, vol. 105, no. 20, Article ID 207201, 2010.

[7] X. G. Xu, H. L. Yang, Y. Wu et al., "Intrinsic room temperature ferromagnetism in boron-doped ZnO," *Applied Physics Letters*, vol. 97, no. 23, Article ID 232502, 2010.

[8] H. L. Yan, X. L. Zhong, J. B. Wang et al., "Cathodoluminescence and room temperature ferromagnetism of Mn-doped ZnO nanorod arrays grown by chemical vapor deposition," *Applied Physics Letters*, vol. 90, no. 8, Article ID 082503, 2007.

[9] L. R. Shah, W. Wang, H. Zhu et al., "Role of dopant, defect, and host oxide in the observed room temperature ferromagnetism: Co-ZnO versus Co-CeO_2," *Journal of Applied Physics*, vol. 105, no. 7, Article ID 07C515, 3 pages, 2009.

[10] L. Q. Liu, B. Xiang, X. Z. Zhang, Y. Zhang, and D. P. Yu, "Synthesis and room temperature ferromagnetism of FeCo-codoped ZnO nanowires," *Applied Physics Letters*, vol. 88, no. 6, Article ID 063104, 2006.

[11] D. Rubi, J. Fontcuberta, A. Calleja, L. Aragonès, X. G. Capdevila, and M. Segarra, "Reversible ferromagnetic switching in ZnO:(Co, Mn) powders," *Physical Review B*, vol. 75, no. 15, Article ID 155322, 2007.

[12] M. Chakrabarti, S. Dechoudhury, D. Sanyal, T. K. Roy, D. Bhowmick, and A. Chakrabarti, "Observation of room temperature ferromagnetism in Mn-Fe doped ZnO," *Journal of Physics D*, vol. 41, no. 13, Article ID 135006, 2008.

[13] Y. Q. Chang, D. B. Wang, X. H. Luo et al., "Synthesis, optical, and magnetic properties of diluted magnetic semiconductor Zn1-xMnxO nanowires via vapor phase growth," *Applied Physics Letters*, vol. 83, no. 19, pp. 4020–4022, 2003.

[14] Z. C. Zhang, B. B. Huang, Y. Q. Yu, and D. L. Cui, "Electrical properties and Raman spectra of undoped and Al-doped ZnO thin films by metalorganic vapor phase epitaxy," *Materials Science and Engineering B*, vol. 86, no. 2, pp. 109–112, 2001.

[15] J. M. Calleja and M. Cardona, "Resonant Raman scattering in ZnO," *Physical Review B*, vol. 16, no. 8, pp. 3753–3761, 1977.

[16] Y. Huang, M. Liu, Z. Li, Y. Zeng, and S. Liu, "Raman spectroscopy study of ZnO-based ceramic films fabricated by novel sol-gel process," *Materials Science and Engineering B*, vol. 97, no. 2, pp. 111–116, 2003.

[17] L. W. Yang, X. L. Wu, G. S. Huang, T. Qiu, and Y. M. Yang, "In situ synthesis of Mn-doped ZnO multileg nanostructures and Mn-related Raman vibration," *Journal of Applied Physics*, vol. 97, no. 1, Article ID 014308, pp. 1–14308, 2005.

[18] C. L. Du, Z. B. Gu, M. H. Lu et al., "Raman spectroscopy of (Mn, Co)-codoped ZnO films," *Journal of Applied Physics*, vol. 99, no. 12, Article ID 123515, 2006.

[19] J. B. Wang, G. J. Huang, X. L. Zhong, L. Z. Sun, Y. C. Zhou, and E. H. Liu, "Raman scattering and high temperature ferromagnetism of Mn-doped ZnO nanoparticles," *Applied Physics Letters*, vol. 88, no. 25, Article ID 252502, 2006.

[20] X. L. Wu, G. G. Siu, C. L. Fu, and H. C. Ong, "Photouminescence and cathodoluminescence studies of stoichiometric and oxygen-deficient ZnO films," *Applied Physics Letters*, vol. 78, no. 16, pp. 2285–2287, 2001.

[21] S. Mochizuki, B. Piriou, and J. Dexpert-Ghys, "Spin-wave-assisted photoluminescence in MnO crystals," *Journal of Physics: Condensed Matter*, vol. 2, no. 23, pp. 5225–5232, 1990.

[22] Y. Q. Chang, D. P. Yu, G. H. Li et al., "Photoluminescence characterization of nanocrystalline ZnO array," *Chinese Physics Letters*, vol. 21, no. 11, pp. 2301–2304, 2004.

[23] S. Ramachandran, J. Narayan, and J. T. Prater, "Effect of oxygen annealing on Mn doped ZnO diluted magnetic semiconductors," *Applied Physics Letters*, vol. 88, no. 24, Article ID 242503, 2006.

[24] H. S. Hsu, J. C. A. Huang, Y. H. Huang et al., "Evidence of oxygen vacancy enhanced room-temperature ferromagnetism in Co-doped ZnO," *Applied Physics Letters*, vol. 88, no. 24, Article ID 242507, 2006.